Highlights

Film Thickness in Elastohydrodynamically Lubricated Slender Elliptic Contacts

Marius Wolf,Sergey Solovyev,Arshia Fatemi

- Benchmarking of analytical film thickness equations for elliptic contacts
- Derivation of new analytical film thickness equation for slender elliptic contacts
- Incorporation of asymptotic solutions for maximisation of validity range
- Excellent agreement with multi-level EHL simulation
- Representation of effect of increasing film thickness with increasing load

Film Thickness in Elastohydrodynamically Lubricated Slender Elliptic Contacts

Marius Wolf*, Sergey Solovyev and Arshia Fatemi

Robert Bosch GmbH, Corporate Sector Research and Advance Engineering, Robert-Bosch-Campus 1, 71272 Renningen, Germany

ARTICLE INFO

Keywords:
Film Thickness
Elastohydrodynamic Lubrication
Elliptic Contacts
Simulation

ABSTRACT

In this paper, analytical equations for the central film thickness in slender elliptic contacts are investigated. A comparison of state-of-the-art formulas with simulation results of a multilevel EHL solver is conducted and shows considerable deviation. Therefore, a new film thickness formula for slender elliptic contacts with variable ellipticity is derived. It incorporates asymptotic solutions, which results in validity over a large parameter domain. It captures the behaviour of increasing film thickness with increasing load for specific very slender contacts. The new formula proves to be significantly more accurate than current equations.

1. Introduction

Fluid film thickness equations are the main bridge between scientific studies on elastohydrodynamic and its engineering applications in gears and rolling element bearings. The first mathematical film thickness formulation for highly concentrated contacts is proposed in the seminal work of Dowson and Higginson for minimum film thickness in 1961 [1] and Dowson and Toyoda for central film thickness [2] both for line contacts. They formulated the dimensionless film thickness H as a function of three dimensionless parameters of material (G), speed (U) and load (W), which were easy to use, physically making sense and are nowadays immensely established in application. Two decades later, Hamrock and Dowson published a series of papers [3–6], regarding elliptic contacts, systematically investigating effects of ellipticity as well as above mentioned parameters. More recently, Lubrecht et al. [7] revisited the equations developed above with higher computational power and finer numerical precision. The investigators have been astonished by confirmation the precision of the equations for line contact developed 50 years prior to their investigation and commented about minor academic issues.

However, before these investigations Ranger et al. [8] at imperial college were the first group who developed a numerical equation for line and point contacts. Yet, their work has not been appreciated because it predicts a counter-intuitive behaviour of increasing film thickness with increasing load within the parameter range of their studies. Recently, this behaviour has been verified and explained [9].

In 1992 Moes [10] adopted the optimum similarity analysis to the domain of lubricated contacts and reduced the number of non-dimensional parameters to two (L and M). By incorporation of asymptotic solutions for different lubrication regimes, the outreach of line contact film thickness equation is extended to isoviscous-elastic, piezoviscous-rigid and isoviscous-rigid regimes. Adopting the methodology of Moes, Nijenbanning et al. [11] solve EHL equations numerically for wide elliptic contacts and for a large number of combinations of M and L, which have been addressed extensively in this paper.

Due to its more widespread application in rolling element bearings, the above mentioned equations focus prevalently on wide elliptic contacts e.g., the entrainment velocity is in the direction of the minor contact ellipse axis. The slender elliptic contacts have been less subject to systematic studies and film thickness equations are not optimised to cover this particular shape of contacts and its domain of parameters. The major significant work on film thickness of slender contacts is based on the extensive study of Chittenden et al. [12, 13] using the same numerical algorithm of Hamrock and Dowson. In addition, Moes [14] adapted the formula of Nijenbanning et al. [11] to general elliptic contacts, however, the deviation between these formulas is negligible. Within this paper, slender contacts are defined as elliptic contact with entrainment velocity directed along the major axis of the contact ellipse. These contacts occur, for example, at

*Corresponding author

marius.wolf2@de.bosch.com (M. Wolf); sergey.solovyev@de.bosch.com (S. Solovyev); arshia.fatemi@de.bosch.com (A. Fatemi)

ORCID(s): 0000-0002-6504-9740 (M. Wolf)

Nomenclature

a	major semi-axis of Hertzian contact ellipse
D	ellipticity ratio
E'	reduced young's modulus, $1/E' = 0.5((1-\nu_1^2)/E_1 + (1-\nu_2^2)/E_2)$
E_i	young's modulus of body i
F_N	normal force
G	dimensionless material parameter (Moes)
$\tilde{H}$	dimensionless film thickness
H	dimensionless film thickness (Moes)
h	film thickness
H_{00}	curvefit parameter
L	dimensionless material parameter
M	dimensionless load parameter (Moes)
p	pressure
R_i	reduced radius of curvature in i direction, $1/R_i = 1/R_{i,1} + 1/R_{i,2}$
s, t	curvefit parameters for isoviscous-piezoviscous transition
U	dimensionless speed parameter
u_0	sum velocity, $u_0 = u_1 + u_2$
u_i	velocity of body i
W	dimensionless load parameter
X	Dimensionless x-direction, $X = x/a$
Y	Dimensionless y-direction, $Y = y/a$
α	Barus parameter
η	viscosity
$\dot{\gamma}$	shear rate
ν_i	poisson's ratio of body i
ρ	mass density
Indices	
0	atmospheric pressure
1,2	body 1, body 2
C	Chittenden
com	compressible
e	entrainment direction
H	Hertzian
IE	isoviscous-elastic
inc	incompressible
IR	isoviscous-rigid
M	regime of increasing film thickness with increasing load parameter
N	Nijenbanning
PE	piezoviscous-elastic
PR	piezoviscous-rigid
s	direction perpendicular to entrainment

the roller-flange interface within cylindrical or tapered roller element bearings or within worm gears and are therefore a highly relevant field of research [15–17].
In this paper the problem of analytical film thickness expressions for slender elliptic contacts is revisited. The focus of this paper is on the central film thickness, since it represents the major part of the contact ellipse and the high pressure region. It is defined as the film thickness at the location of maximum fluid pressure [11, 14].

2. Simulation Model

The EHL simulations were performed with a multilevel EHL solver analogous to the work of Venner [18]. Detailed descriptions of the working principle of EHL solvers can be found in the literature [19, 20] and are therefore not given here.
The following assumptions are made:

- fluid incompressibility
- smooth surfaces / no solid contact
- steady state
- isothermal behaviour
- fully-flooded contact / no starvation
- Newtonian behaviour

- Barus pressure-viscosity law

The Newtonian ($\eta \neq \eta(\dot{\gamma})$) and Barus

$$\eta(p) = \eta_0 \exp(\alpha p) \tag{1}$$

modelling of the fluid hold valid, since the film thickness is solely dependent on the condition of the fluid at the inlet of the contact.
As shown by Moes [10], the problem can be reduced to the dimensionless parameters

$$H = \frac{h}{R_\mathrm{e}} \left(\frac{\eta_0 u_0}{E' R_\mathrm{e}} \right)^{-1/2} \tag{2}$$

$$M = \frac{F_\mathrm{N}}{E' {R_\mathrm{e}}^2} \left(\frac{\eta_0 u_0}{E' R_\mathrm{e}} \right)^{-3/4} \tag{3}$$

$$L = \alpha E' \left(\frac{\eta_0 u_0}{E' R_\mathrm{e}} \right)^{1/4}. \tag{4}$$

These parameters and the ellipticity parameter, defined as the ratio of the reduced radii of curvature,

$$D = \frac{R_\mathrm{e}}{R_\mathrm{s}} \tag{5}$$

are used for contact characterization within this paper. R_e and R_s represent the effective radii in direction of entrainment velocity (R_e) and perpendicular to it (R_s). The effective radius in direction i can be calculated via

$$1/R_i = 1/R_{i,1} + 1/R_{i,2}. \tag{6}$$

Furthermore, the dimensionless spatial directions

$$X = \frac{x}{a} \tag{7}$$

$$Y = \frac{y}{a} \tag{8}$$

with a as the major semi-axis of the Hertzian contact ellipse are introduced for post-processing the film thickness distributions. A detailed definition of the variables can be found in the nomenclature.

3. State-of-the-art formulas

Following the pioneer work of Hamrock and Dowson [5] in 1977, many more analytical film thickness formulas for point and elliptic contacts were derived [10–12, 21–25]. A comprehensive overview is given by Marian et al. [26] and Van Leeuwen [27], which also provides a comparison to experimental data.
However, almost all approaches focus on point ($D = 1$) or wide elliptic contacts ($D < 1$). Only Chittenden et al. [12] consider slender contacts ($D > 1$). The authors also provides an analytical formula for arbitrary entrainment angles [22]. It is more commonly used in literature and is therefore benchmarked against EHL simulations. In order to investigate, whether or not analytical formulas for wide contacts can be extrapolated to slender contacts, the film thickness formula of Nijenbanning et al. [11] is reviewed as well. This formula is chosen, since it integrates the asymptotic behaviour and is therefore expected to be valid for a greater range of parameters compared to other approaches.

3.1. Chittenden et al. [22]

Chittenden uses the dimensionless parameters

$$U = \frac{\eta_0 u_0}{2 E' R_\mathrm{e}} \tag{9}$$

$$G = \alpha E' = L(2U)^{-1/4} \tag{10}$$

$$W = \frac{F_{\mathrm{N}}}{E' {R_{\mathrm{e}}}^2} = M(2U)^{3/4} \tag{11}$$

and

$$\tilde{H}_{\mathrm{C}} = \frac{h}{R_{\mathrm{e}}} = H(2U)^{1/2}. \tag{12}$$

The film thickness formula for arbitrary entrainment angels reads

$$\tilde{H}_{\mathrm{C}} = 4.31 G^{0.49} U^{0.68} W^{-0.073} \left[1 - \exp\left(-1.23 \left(\frac{R_{\mathrm{s}}}{R_{\mathrm{e}}} \right)^{\frac{2}{3}} \right) \right]. \tag{13}$$

It must be noted that Chittenden [22] is using training data obtained by simulations with compressible fluids and Roelands [28] behaviour for the pressure-viscosity relationship. While the kind of used pressure-viscosity law has no significant effect on film thickness, (in)compressibility must be considered, when comparing different approaches. Therefore, correction via

$$H_{\mathrm{com}} = \frac{H_{\mathrm{inc}}}{\bar{\rho}(p_{\mathrm{H}})} \tag{14}$$

with the pressure-density law of Dowson and Higginson [29, 30]

$$\bar{\rho}(p) = \frac{\rho(p)}{\rho_0} = \frac{5.9 \times 10^8 + 1.34p}{5.9 \times 10^8 + p} \tag{15}$$

is used [25]. p_{H} refers to the maximum Hertzian pressure in Pa.
For comparison, H as defined by Moes [10] from eq. 2 is used. Therefore, $\tilde{H}_{\mathrm{C}}$ from eq. 13 is multiplied by $(2U)^{-1/2}$ beforehand.

3.2. Nijenbanning et al. [11]

The film thickness formula of Nijenbanning et al. [11] is based on the same assumptions as stated in sect. 2. It was derived for wide elliptic contacts ($D < 1$) and reads:

$$H_{\mathrm{N}} = \left\{ \left[H_{\mathrm{N,IR}}^{1.5} + \left(H_{\mathrm{N,IE}}^{-4} + H_{\mathrm{N,00}}^{-4} \right)^{-3/8} \right]^{2s/3} + \left[H_{\mathrm{N,PE}}^{-8} + H_{\mathrm{N,PR}}^{-8} \right]^{-s/8} \right\}^{1/s} \tag{16}$$

with

$$H_{\mathrm{N,IR}} = 145 \left(1 + 0.796 D^{14/15} \right)^{-15/7} D^{-1} M^{-2} \tag{17}$$

$$H_{\mathrm{N,IE}} = 3.18 \left(1 + 0.006 \ln(D) + 0.63 D^{4/7} \right)^{-14/25} D^{-1/15} M^{-2/15} \tag{18}$$

$$H_{\mathrm{N,PR}} = 1.29 \left(1 + 0.691 D \right)^{-2/3} L^{2/3} \tag{19}$$

$$H_{\mathrm{N,PE}} = 1.48 \left(1 + 0.006 \ln(D) + 0.63 D^{4/7} \right)^{-7/20} D^{-1/24} M^{-1/12} L^{3/4} \tag{20}$$

$$H_{\mathrm{N,00}} = 1.8 D^{-1} \tag{21}$$

$$s = 1.5 \left[1 + \exp\left(-1.2 \frac{H_{\mathrm{N,IE}}}{H_{\mathrm{N,IR}}} \right) \right]. \tag{22}$$

3.3. Benchmarking

First, the presented film thickness formulas are tested for wide elliptic contacts in order to evaluate both the quality of the film thickness formulas and the quality of the used EHL solver. The results are shown for different values of M and L and an ellipticity ratio of $D = 0.25$ in fig. 1.
It can be seen that the formula of Chittenden et al. [22] (eq. 13) only shows partial consistency for medium values of M and medium to large values of L. It fails to predict the film thickness for small values of both M and L. This

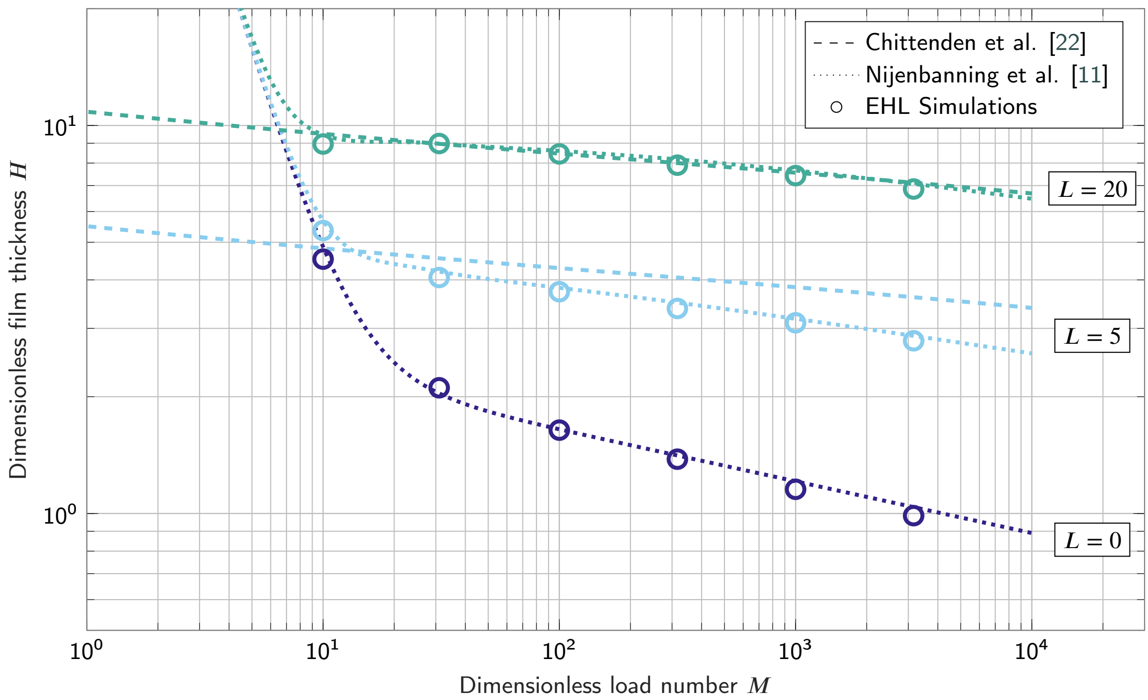

Figure 1: Benchmarking of state-of-the-art film thickness formulas for wide elliptic contacts ($D = 0.25$).

becomes especially evident for the case of $L = 0$: Eq. 13 predicts $H = 0$, which is clearly not the case.
This comparison does not claim to be an exhaustive evaluation of the film thickness formula of Chittenden et al. [22]. Instead, it investigates its general capability to predict the film thickness in elliptic contacts. For a complete evaluation, results of EHL simulations with compressible fluids instead of correction via eq. 14 are required.
In contrast, excellent agreement with a slight tendency towards overestimation is given between the EHL simulations and the formula of Nijenbanning et al. [11]. Especially the asymptotic behaviour for $L = 0$ and $M \to 0$ is captured in a superior way compared to Chittenden et al. [22]. The precise conformity between Nijenbanning et al. [11] and the employed EHL solver is a strong indication for correct functioning of the EHL solver.
Wheeler et al. [13] observe a significant systematic overestimation of the film thickness by the formula of Nijenbanning et al. [11]. This contradicts the findings of this paper. However, the overestimation occurred, when comparing the Nijenbanning formula with compressible EHL simulations. Since the model of Nijenbanning et al. [11] assumes incompressibility, the overestimation is explainable and expected.
Following the benchmarking of wide elliptic contacts, the film thickness formulas are also evaluated for slender elliptic contacts. The results for a wide range of M and L values are shown in fig. 2 ($D = 2$) and fig. 3 ($D = 5$). As for wide elliptic contacts, the formula of Chittenden et al. [22] only correctly captures the behaviour for medium values of both M and L. The quality of the prediction of Nijenbanning et al. [11] declines with increasing ellipticity as a result of stronger extrapolation from its training range.
This comparison demonstrates the necessity of a new film thickness formula for slender elliptic contacts with validity over a broad parameter domain.

4. New Film Thickness Formula for Slender Contacts

The focus of this paper is to provide an easy-to-implement formula by using standard mathematical functions. Johnson [31] distinguishes four different lubrication regimes:

1. Isoviscous-Rigid (small L and small M)
2. Isoviscous-Elastic (small L and large M)
3. Piezoviscous-Rigid (large L and small M)

4. Piezoviscous-Elastic (large L and large M)

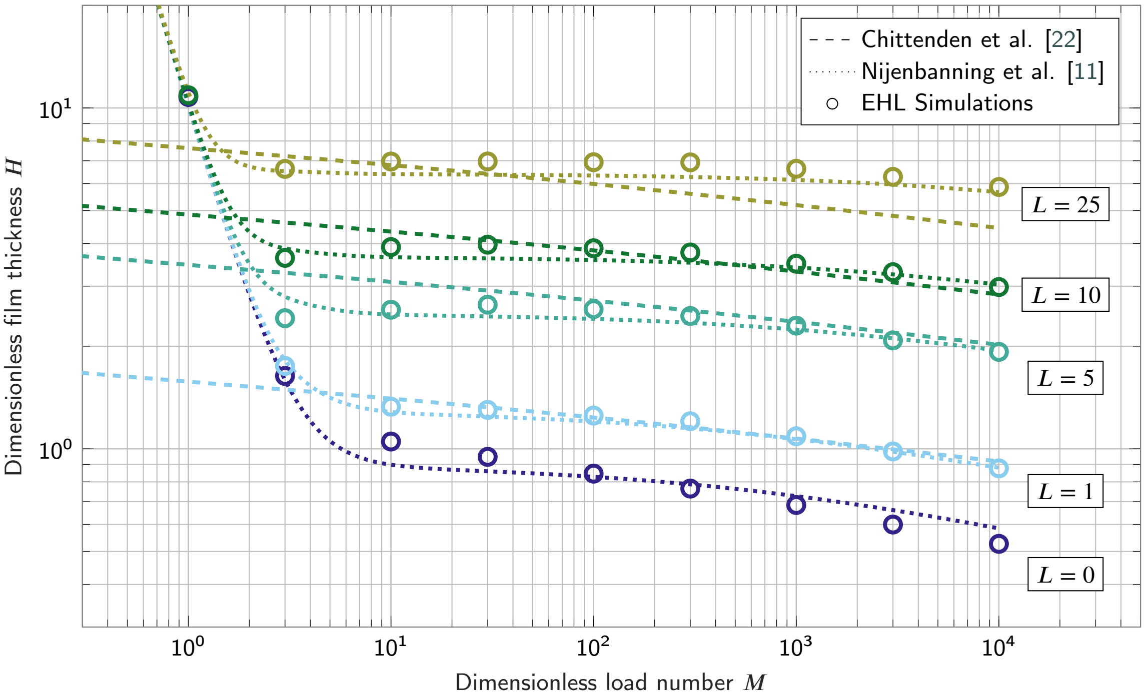

Figure 2: Benchmarking of state-of-the-art film thickness formulas for an ellipticity ratio of $D = 2$.

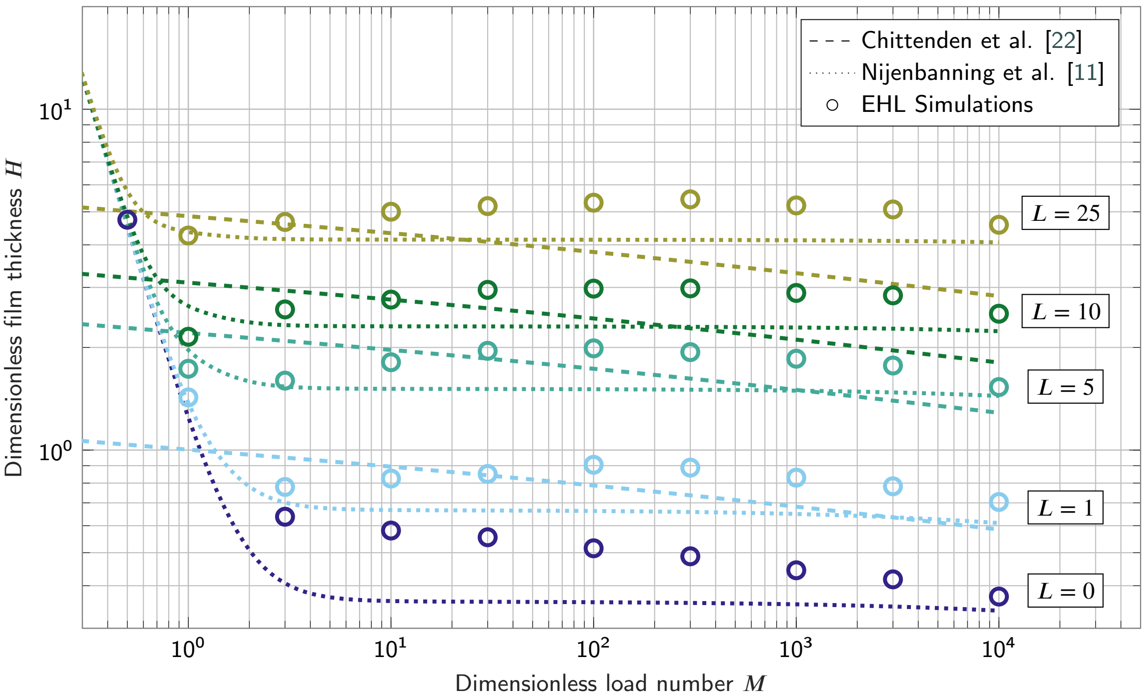

Figure 3: Benchmarking of state-of-the-art film thickness formulas for an ellipticity ratio of $D = 5$.

Unlike for line contacts, the boundaries of the regime cannot be specified explicitly, since they depend on the ellipticity ratio D of the contact.
Solutions for the asymptotic behaviour of the film thickness in a point contact exist for each regime and are incorporated in the film thickness formula. The prefactors C_i of the asymptotic solutions are functions of the ellipticity ratio D and are derived by curve fitting a large number of simulations within each regime, resulting in an overall number of 2282 successfully converged simulations. The base form of each prefactor function is chosen individually to best match the ellipticity dependence. The coefficient were determined using a least squares regression approach.
The dimensionless values L, M and the ellipticity ratio D were varied within $L \in [0, 100], M \in [0.5, 20000]$ and $D \in [1, 10]$. In order to avoid numerical influences on the quality of the simulation results, first the mesh density is increased until no significant change in the central film thickness can be observed any more. Afterwards, the simulation area is increased until again no change in the central film thickness occurs. It should be noted that for simulations with small M values, the required simulation area is many times larger than the Hertzian contact area, whereas for high M values a fine mesh is required.
The final form of the film thickness equation is analogous to Nijenbanning et al. [11]. It is a weighting of the contributions of different lubrication regimes and reads:

$$H = \left\{ \left[H_{\mathrm{IR}}^{1.73} + \left(H_{\mathrm{IE}}^{-1.33} + H_{00}^{-1.33} \right)^{-\frac{1.73}{1.33}} \right]^{\frac{t}{1.73}} + \left[H_{\mathrm{PE}}^{-13.8} + \left(H_{\mathrm{PR}}^{-24.1} + H_{\mathrm{M}}^{-24.1} \right)^{\frac{13.8}{24.1}} \right]^{-\frac{t}{13.8}} \right\}^{1/t} \tag{23}$$

with

$$H_{00} = 4.13 \cdot D^{-1} \tag{24}$$

$$t = \left[\left(1.43^{0.803} + \left(\frac{4.65}{M} \right)^{0.803} \right)^{-\frac{5}{0.803}} + 4^{-5} \right]^{-1/5} \tag{25}$$

as the transition parameters between the isoviscous-rigid and isoviscous-elastic (H_{00}) and between the isoviscous and piezoviscous regimes (t). The coefficients for weighting are based on simulations in between the lubrication regimes. The partial solutions $H_{\mathrm{IR}}, H_{\mathrm{IE}}, H_{\mathrm{PR}}, H_{\mathrm{M}}$ and H_{PE} are defined in the following sections.

4.1. Isoviscous-Rigid

The load-free zone of roller element bearings is an example for the occurrence of isoviscous-rigid contacts. From a similarity analysis follows [11]

$$H_{\mathrm{IR}} \propto M^{-2}. \tag{26}$$

Curve fitting the prefactor C_{IR} leads to

$$H_{\mathrm{IR}} = C_{\mathrm{IR}}(D) \cdot M^{-2} \tag{27}$$

with

$$C_{\mathrm{IR}}(D) = 236 \left(1 + 0.65 D^{0.704} \right)^{-3.37} D^{-1}. \tag{28}$$

A representative film thickness distribution for isoviscous-rigid contacts is given in fig. 4. Although the height profile is similar to the undeformed profile, a slight shift towards the outlet of the contact zone can be observed.

4.2. Isoviscous-Elastic

Contacts including seals, polymer gears or the roller-cage interface are representative of the isoviscous-elastic regime. The asymptotic solution [32, 33]

$$H_{\mathrm{IE}} = C_{\mathrm{IE}}(D) \cdot M^{-2/15} \tag{29}$$

can be curve fitted with

$$C_{\mathrm{IE}}(D) = -0.916 \ln \left(439 \left(\frac{1}{439} + D^{-1} \right) \right) + 7.98 D^{-0.192} \tag{30}$$

to represent slender elliptic contacts.
Fig. 5 shows a typical film thickness distribution for isoviscous-elastic contacts. It can be seen that - unlike in fig. 4 - a significant elastic deformation occurs. However, no plateau is formed.

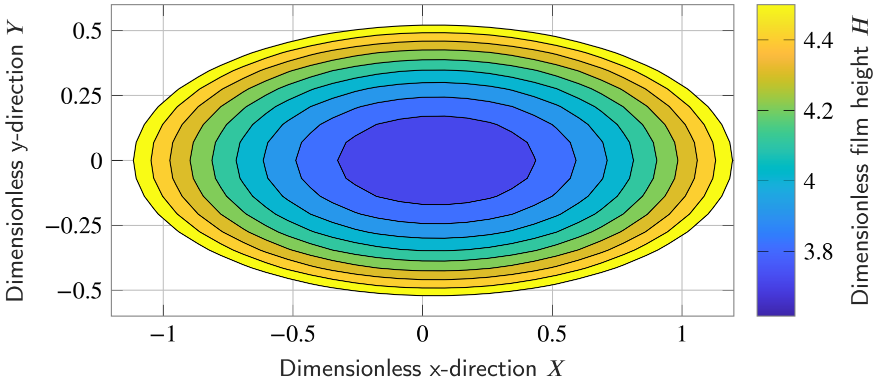

Figure 4: Distribution of the dimensionless film thickness H for a slender isoviscous-rigid contact with $M = 0.5$, $L = 0$ and $D = 5$.

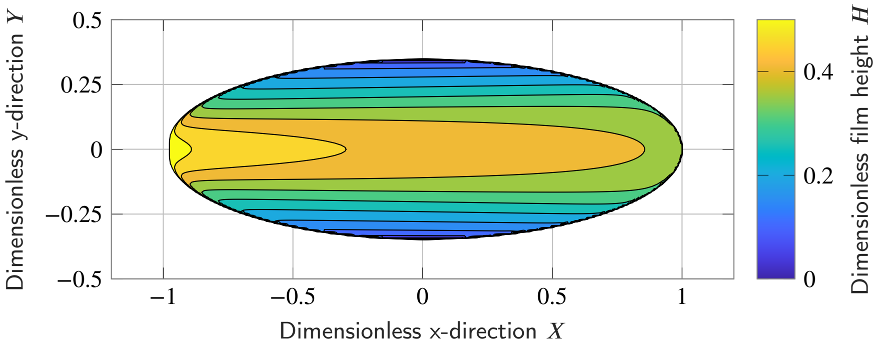

Figure 5: Distribution of the dimensionless film thickness H for a slender isoviscous-elastic contact with $M = 7500$, $L = 0$ and $D = 5$.

4.3. Piezoviscous-Rigid

Based on the work of Grubin [34], the following formula can be derived for the piezoviscous-rigid regime:

$$H_{\mathrm{PR}} = C_{\mathrm{PR}}(D) \cdot L^{2/3} \tag{31}$$

with

$$C_{\mathrm{PR}}(D) = 0.441 \ln\left(-0.258\left(-\frac{1}{0.258} + D^{-1}\right)\right) + 1.11 D^{-0.332}. \tag{32}$$

For very slender contacts, a counter-intuitive behaviour of the film thickness can be observed: The film thickness increases with increasing load [35]. This effect takes place for piezoviscous lubricants and small to medium loads and can be observed, for example in fig. 12. It is caused by an increased contact ellipse, which reduces side-leakage of the lubricant.

Eq. 31 cannot account for this behaviour. Therefore, a new partial solution for this regime was derived:

$$H_{\mathrm{M}} = C_{\mathrm{M}}(D) \cdot L^{2/3} M^{0.0931-0.00072L} \tag{33}$$

with

$$C_{\mathrm{M}}(D) = -82.1 \ln\left(0.00618\left(\frac{1}{0.00618} + D^{-1}\right)\right) + 1.41 D^{-0.528}. \tag{34}$$

Eq. 33 represents contacts in between the isoviscous-rigid and the piezoviscous-rigid regime (see fig. 9). Its capability to correctly capture the physical behaviour is demonstrated by a detail analysis in fig. 6.

A reference film thickness distribution for piezoviscous-rigid contacts is given in fig. 7. It can be seen that a relatively narrow plateau, which is bounded by pronounced minima of the film thickness, has formed.

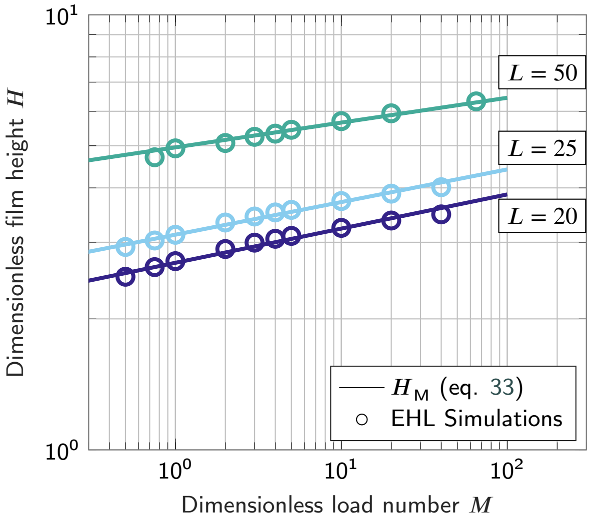

Figure 6: Validation of partial solution H_{M} (eq. 33) for regime of increasing H with increasing M for $D = 10$.

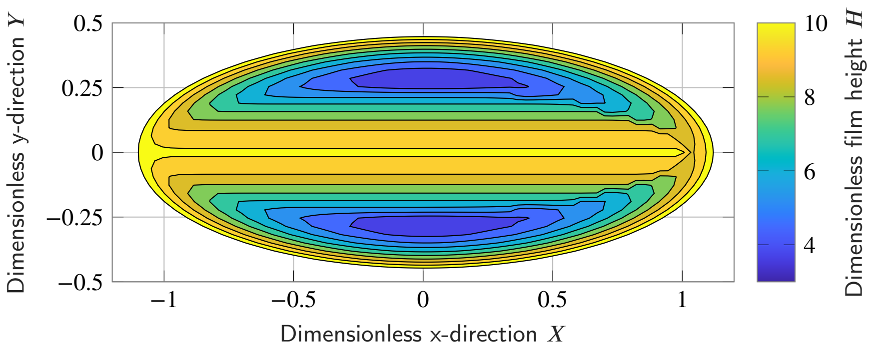

Figure 7: Distribution of the dimensionless film thickness H for a slender piezoviscous-rigid contact with $M = 100$, $L = 60$ and $D = 5$.

4.4. Piezoviscous-Elastic

Piezoviscous-elastic contacts occur, for example, in the load-zone of roller element bearings or within highly loaded gears. The asymptotic solution of this regime for point contacts of Grubin [34]

$$H_{\mathrm{PE}} = C_{\mathrm{PE}}(D) \cdot L^{3/4} M^{-1/12} \tag{35}$$

can be generalised for slender contacts with

$$C_{\mathrm{PE}}(D) = 0.205 \ln\left(439\left(\frac{1}{439} + D^{-1}\right)\right). \tag{36}$$

As can be seen in fig. 8, a relatively wide plateau and a constant film thickness in entrainment direction are characteristic of piezoviscous-elastic contacts.

4.5. Discussion

The final formula for the film thickness (eq. 23) is a weighting of the contribution of different lubrication regimes. An example for the contributions of each regime towards the overall film thickness is given in fig. 9. As the load parameter M increases, it can be seen how H follows different partial solutions. Note the contributions shown in fig. 9 only represent the exemplary case of $L = 15$ and $D = 10$ and cannot be generalised.
The herein presented formula has been developed using an analogous methodology as Nijenbanning et al. [11]. Both

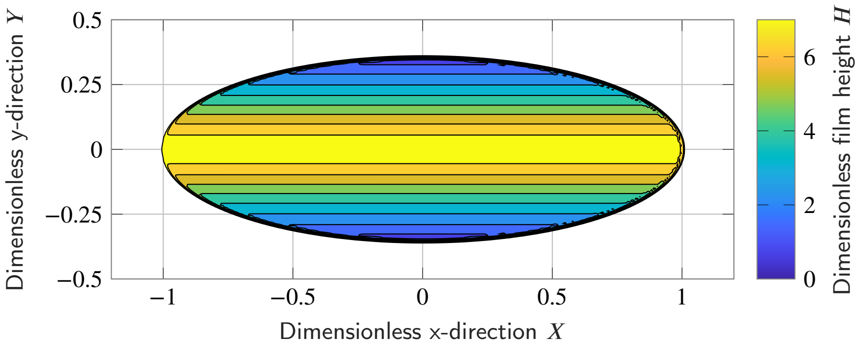

Figure 8: Distribution of the dimensionless film thickness H for a slender piezoviscous-elastic contact with $M = 10000$, $L = 40$ and $D = 5$.

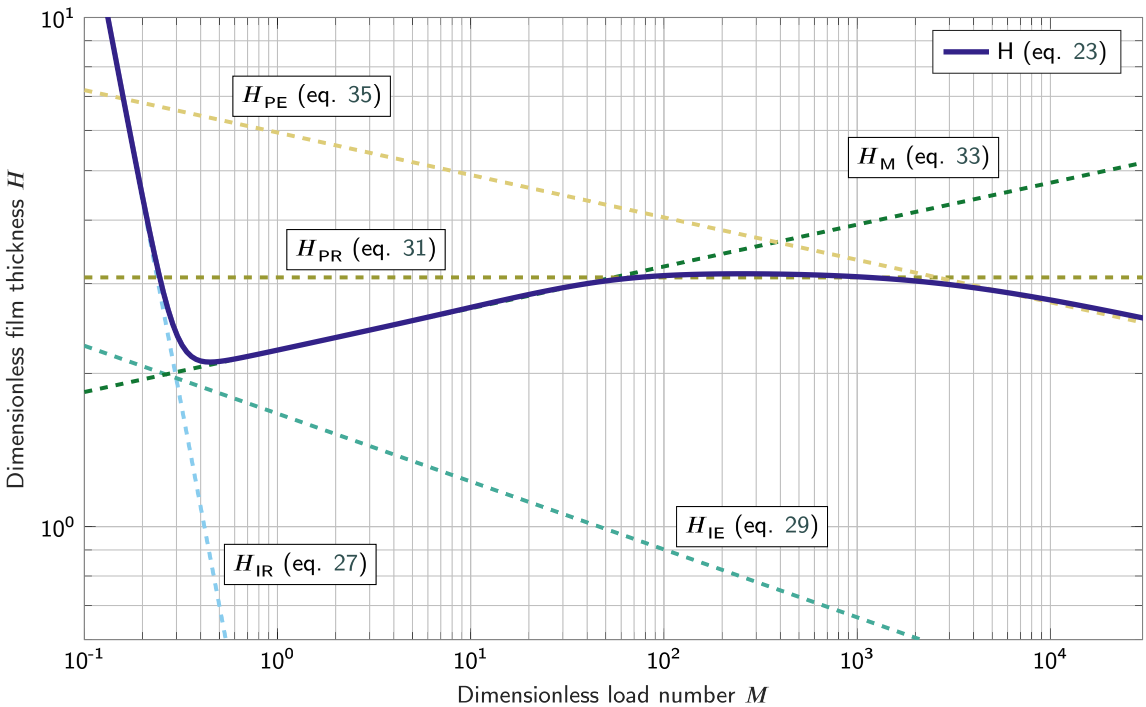

Figure 9: Contributions of the different lubrication regimes to the overall film thickness according to eq. 23, for $L = 15$ and $D = 10$.

formulas were derived for entrainment along a specific axis of the contact ellipse and do not claim to be valid for entrainment along the other axis. Nevertheless, the point contact problem ($D = 1$), as the transition between wide and slender elliptic contacts, can be calculated with both formulas.

For this reason, the predictions of both formulas are compared and plotted in fig. 10. It can be seen that the overall agreement of both formulas is very good. Yet, the formulas diverge at the transition from the isoviscous-rigid to the neighbouring regimes ($M \in [5, 20]$) and within the isoviscous-elastic regime ($L = 0$).

The asymptotic solution of the film thickness of elliptic contact for $D \to 0$ corresponds to the solution of the line contact problem. Yet, to the best of the author's knowledge, no such solution exists in the literature for $D \to \infty$. However, a steady decrease of the film thickness with increasing ellipticity can be observed. Physically, this can be explained by an increasing side-leakage of the fluid resulting from a shrinking minor axis of the contact ellipse [35]. This behaviour also shows in the prefactors C_i, which are monotonically decreasing functions. The theoretical case of $D = \infty$ cannot be simulated. Nonetheless, following the outlined path of reasoning, it is expected that no fluid film

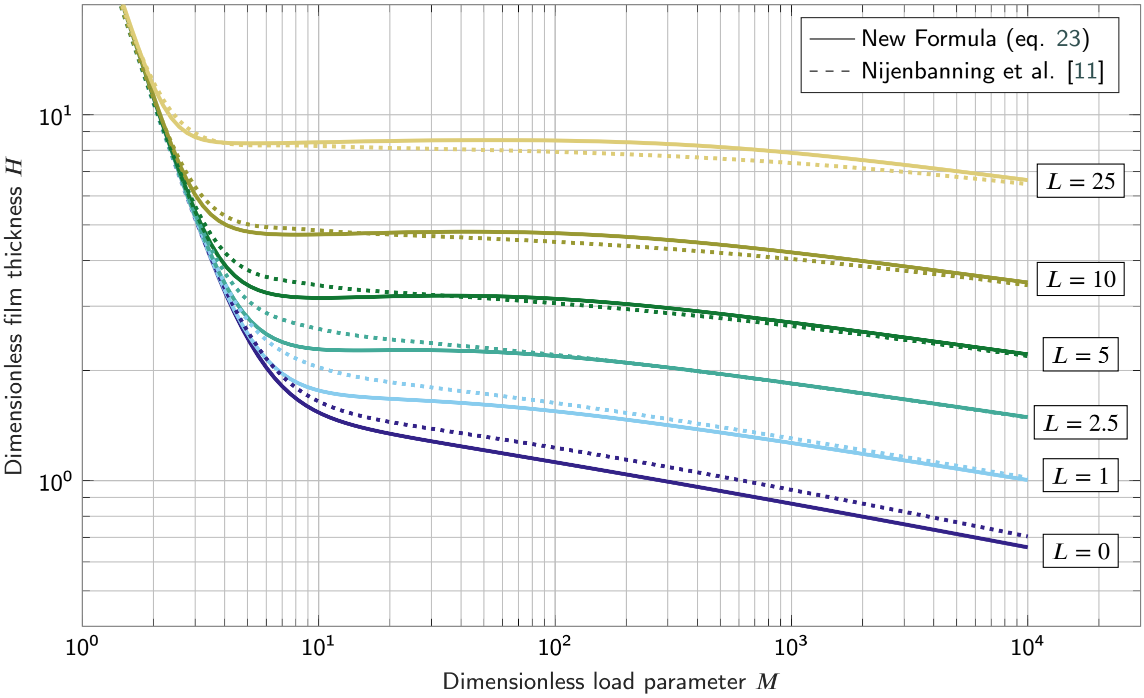

Figure 10: Comparison of the new film thickness formula (eq. 23) against the formula of Nijenbanning [11] for point contacts ($D = 1$).

formation occurs and it follows

$$\lim_{D\to\infty} h(D) = 0. \tag{37}$$

This behaviour is incorporated in the new film thickness formula, since

$$\lim_{D\to\infty} C_i(D) = 0. \tag{38}$$

Additionally, a shift of the lubrication regimes towards smaller values of M with increasing D can be observed (see, for example, fig. 11 and fig. 12).

The newly derived equation is the first analytical film thickness formula for slender elliptic contacts to represent the regime of increasing film thickness with increasing load parameter M. The necessity of this detailedness, as well as the incapability of state-of-the-art formulas to capture this behaviour, can be seen very well in fig. 12.

5. Discussion on Regression Error

The training error of the newly developed film thickness formula for slender elliptic contacts (eq. 23) is 1.43 %. It is defined as the relative difference between predictions of the new formula (eq. 23) and results of EHL simulations used to obtain this equation.

Since the training error is not sufficient to estimate the quality of the new formula, it is also tested against 100 random EHL simulations. The test parameters were obtained using a latin hypercube sampling algorithm. The tested parameter range is $M \in [0.5, 10000]$, $L \in [0, 40]$ and $D \in [1, 20]$. The fluid properties, velocities and radii resulting in the dimensionless parameters M, L and D were modified for the training simulations. Due to the high computational cost of EHL simulations, only 100 were performed for testing.

The average test error is 1.34 % and the maximum test error corresponds to 4.36 %. The fact that the test and training error are almost identical is a clear indication that the number of training data points (2282) is sufficient and no overfitting occurs.

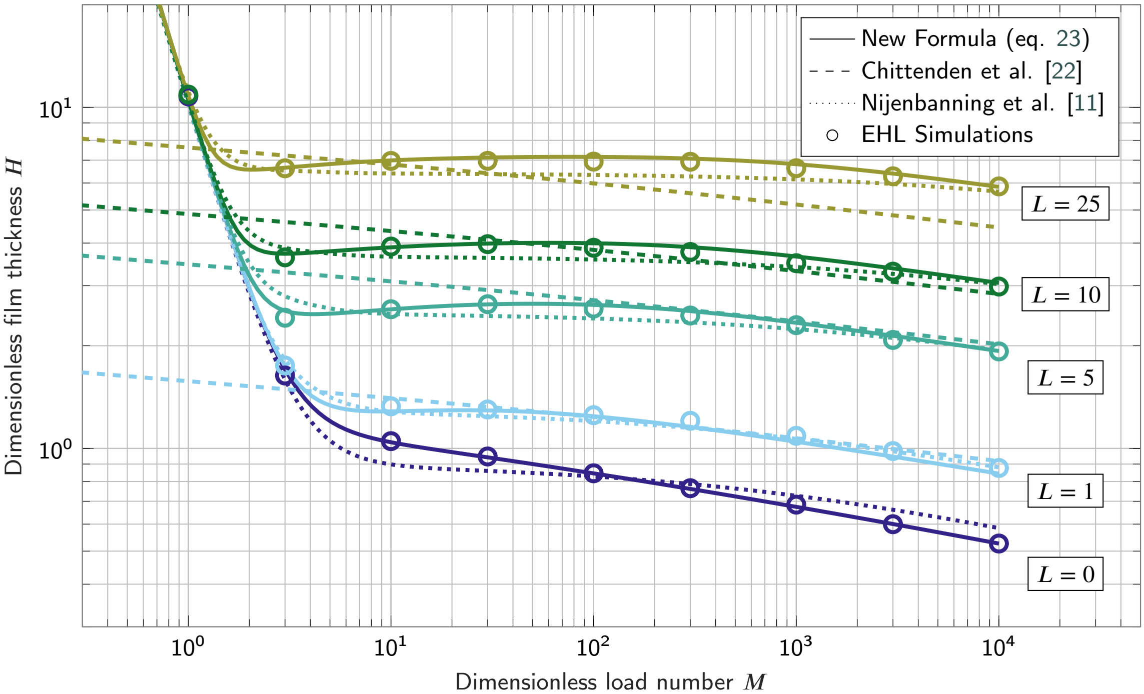

Figure 11: Comparison of the new film thickness equation (eq. 23) against the film thickness formulas of Chittenden et al. [12] and Nijenbanning et al.[11] for an ellipticity ratio of $D = 2$.

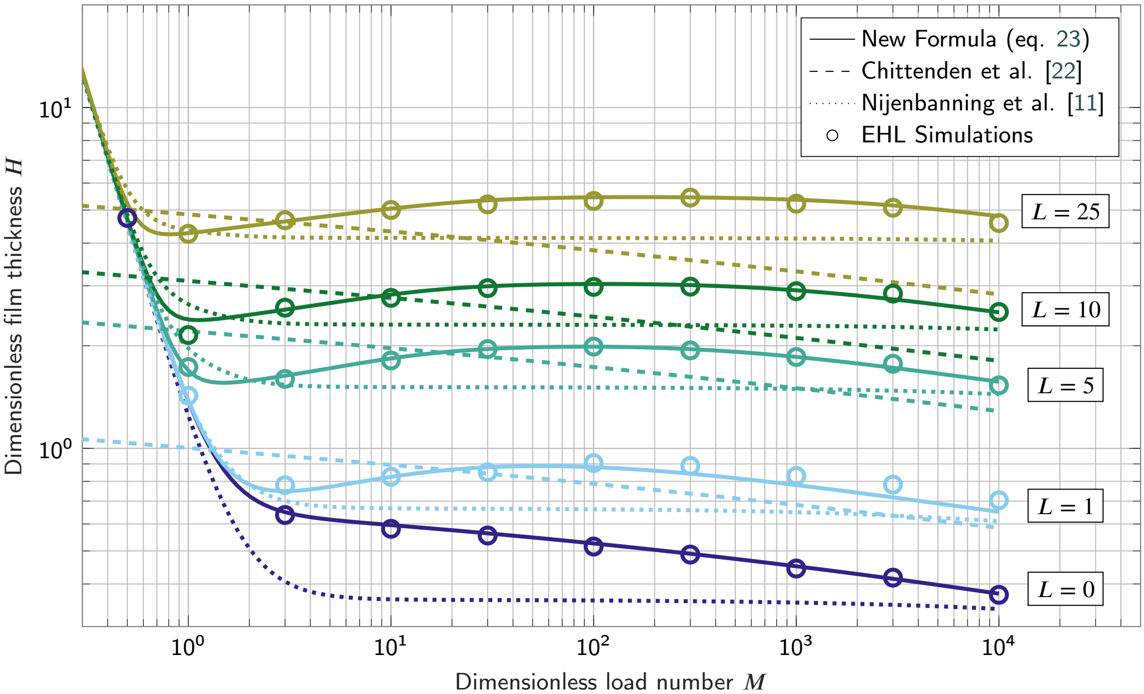

Figure 12: Comparison of the new film thickness equation (eq. 23) against the film thickness formulas of Chittenden et al. [12] and Nijenbanning et al.[11] for an ellipticity ratio of $D = 5$.

The range of tested ellipticity values ($D \in [1, 20]$) extended the training range ($D \in [1, 10]$). The average test error for simulations with $D > 10$ was 2.54 % (max. 3.98 %). This shows that the quality of the newly derived formula declines when being extrapolated to even more slender contacts. However, it can still predict the film thickness solidly. Extrapolation of M and L was not tested, since convergence would have been critical, especially for more extreme values of M.
The superior quality of the new film thickness formula in comparison to the approaches of Chittenden [12] and Nijenbanning [11] can also be seen in fig. 11 and fig. 12. It must be emphasised that the shown EHL simulation results were not part of the training set of this study.

6. Conclusion

State-of-the-art analytical central film thickness equations were benchmarked for elliptic contacts with entrainment along the major axis of the contact ellipse (slender contacts) against multi-level EHL simulations. The results show an unambiguous necessity for an improved analytical formula with validity over a great parameter domain.
Therefore, a new analytical central film thickness formula for slender elliptic contacts was developed. Asymptotic solutions for each lubrication regime are the basis of the film thickness equation. The main advantages of the new formula are

- large number of training data (2282 simulations)
- wide range of ellipticity ratios ($D \in [1, 10]$) has been adopted
- no limitation on L and M parameter domain by incorporation of asymptotic solutions
- agreement with EHL simulations (avg. test error of 1.34 %)
- improved prediction quality compared to literature film thickness equations [11, 22]
- first formula to incorporate the effect of rising film thickness with increasing load

Declaration of competing interest

The authors declare that they have no known competing financial interests or personal relationships that could have appeared to influence the work reported in this paper.

Funding

This research did not receive any specific grant from funding agencies in the public, commercial, or not-for-profit sectors.

Acknowledgements

The authors would like to thank Prof. Dr. Gerhard Poll (University of Hannover) for his advice on state-of-the-art film thickness formulas and film formation in EHL contacts. Patrick Stuhler and Dr. Nadine Nagler (both Bosch Rexroth AG) are acknowledged for helpful discussions and their general support.

References

[1] Dowson D, Higginson GR. New Roller Bearing Lubrication Formula. Engineering. 1961;192:158–159.
[2] Dowson D, Toyoda S. A Central Film Thickness Formula for Elastohydrodynamic Line Contacts. Proceedings of the Fifth Leeds-Lyon Symposium on Tribology. 1978;p. 60–64.
[3] Hamrock BJ, Dowson D. Isothermal Elastohydrodynamic Lubrication of Point Contacts: Part I—Theoretical Formulation. Journal of Lubrication Technology. 1976;98(2):223–228.
[4] Hamrock BJ, Dowson D. Isothermal Elastohydrodynamic Lubrication of Point Contacts: Part II—Ellipticity Parameter Results. Journal of Lubrication Technology. 1976;98(3):375–381.
[5] Hamrock BJ, Dowson D. Isothermal elastohydrodynamic lubrication of point contacts: part III—fully flooded results. Journal of Lubrication Technology. 1977;99(2):264–275.

[6] Hamrock BJ, Dowson D. Isothermal elastohydrodynamic lubrication of point contacts: Part IV — starvation results. Journal of Lubrication Technology. 1977;99(1):15–23. Available from: https://doi.org/10.1115/1.3452973.

[7] Lubrecht AA, Venner CH, Colin F. Film thickness calculation in elasto-hydrodynamic lubricated line and elliptical contacts: The Dowson, Higginson, Hamrock contribution. Proceedings of the Institution of Mechanical Engineers, Part J: Journal of Engineering Tribology. 2009;223(3):511–515. Available from: https://doi.org/10.1243/13506501JET508.

[8] Ranger AP, Ettles CMM, Cameron A. The Solution of the Point Contact Elasto-Hydrodynamic Problem. Proceedings of the Royal Society of London Series A, Mathematical and Physical Sciences. 1975;346(1645):227–244. Available from: http://www.jstor.org/stable/78929.

[9] Zhu D, Wang Q. Elastohydrodynamic Lubrication: A Gateway to Interfacial Mechanics - Review and Prospect. Journal of Tribology. 2011 10;133.

[10] Moes H. Optimum similarity analysis with applications to elastohydrodynamic lubrication. Wear. 1992;159(1):57 – 66. Available from: http://www.sciencedirect.com/science/article/pii/004316489290286H.

[11] Nijenbanning G, Venner CH, Moes H. Film thickness in elastohydrodynamically lubricated elliptic contacts. Wear. 1994;176(2):217 – 229. Available from: http://www.sciencedirect.com/science/article/pii/0043164894901503.

[12] Chittenden RJ, Dowson D, Dunn JF, Taylor CM, Johnson KL. A theoretical analysis of the isothermal elastohydrodynamic lubrication of concentrated contacts. I. Direction of lubricant entrainment coincident with the major axis of the Hertzian contact ellipse. Proceedings of the Royal Society of London A Mathematical and Physical Sciences. 1985;397(1813):245–269. Available from: https://royalsocietypublishing.org/doi/abs/10.1098/rspa.1985.0014.

[13] Wheeler JD, Vergne P, Fillot N, Philippon D. On the relevance of analytical film thickness EHD equations for isothermal point contacts: Qualitative or quantitative predictions? Friction. 2016;4(4):369–379.

[14] Moes H. Lubrication and Beyond. Enschede: University of Twente; 2000.

[15] Venner CH, Lubrecht AA. Revisiting film thickness in slender elasto-hydrodynamically lubricated contacts. Proceedings of the Institution of Mechanical Engineers, Part C: Journal of Mechanical Engineering Science. 2010;224(12):2549–2558. Available from: https://doi.org/10.1243/09544062JMES2316.

[16] Kaneta M, Kawashima R, Masuda S, Nishikawa H, Yang P, Wang J. Thermal effects on the film thickness in elliptic EHL contacts with entrainment along the major contact axis. Journal of Tribology. 2002 Apr;124(2):420–427. Available from: https://doi.org/10.1115/1.1430675.

[17] Wolf M, Sanner A, Fatemi A. A semi-analytical approach for rapid detection of roller-flange contacts in roller element bearings. Proc Inst Mech Eng, Part J. 2020;Available from: https://doi.org/10.1177/1350650120964295.

[18] Venner CH, Napel W. Multilevel solution of the elastohydrodynamically lubricated circular contact problem Part I: Theory and numerical algorithm. Wear. 1992;152(2):351 – 367. Available from: http://www.sciencedirect.com/science/article/pii/004316489290132R.

[19] Venner CH, Lubrecht AA. Multi-level methods in lubrication. 1st ed. Dowson D, editor. Elsevier; 2000.

[20] Wang W. EHL, Full Numerical Solution Methods. In: Wang QJ, Chung YW, editors. Encyclopedia of Tribology. Boston, MA: Springer US; 2013. p. 852–859. Available from: https://doi.org/10.1007/978-0-387-92897-5_630.

[21] Venner CH, Napel W. Multilevel solution of the elastohydrodynamically lubricated circular contact problem part II: Smooth surface results. Wear. 1992;152(2):369 – 381. Available from: http://www.sciencedirect.com/science/article/pii/004316489290133S.

[22] Chittenden RJ, Dowson D, Dunn JF, Taylor CM, Johnson KL. A theoretical analysis of the isothermal elastohydrodynamic lubrication of concentrated contacts. II. General case, with lubricant entrainment along either principal axis of the Hertzian contact ellipse or at some intermediate angle. Proceedings of the Royal Society of London A Mathematical and Physical Sciences. 1985;397(1813):271–294. Available from: https://royalsocietypublishing.org/doi/abs/10.1098/rspa.1985.0015.

[23] Evans HP, Snidle RW. The Isothermal Elastohydrodynamic Lubrication of Spheres. Journal of Lubrication Technology. 1981 10;103(4):547–557. Available from: https://doi.org/10.1115/1.3251734.

[24] Masjedi M, Khonsari MM. On the effect of surface roughness in point-contact EHL: Formulas for film thickness and asperity load. Tribology International. 2015 Feb;82:228–244. Available from: http://www.sciencedirect.com/science/article/pii/S0301679X1400334X.

[25] Canzi A, Venner CH, Lubrecht AA. Film thickness prediction in elastohydrodynamically lubricated elliptical contacts. Proc Inst Mech Eng, Part J. 2010;224(9):917–923. Available from: https://doi.org/10.1243/13506501JET717.

[26] Marian M, Bartz M, Wartzack S, Rosenkranz A. Non-Dimensional Groups, Film Thickness Equations and Correction Factors for Elastohydrodynamic Lubrication: A Review. Lubricants. 2020;8(10). Available from: https://www.mdpi.com/2075-4442/8/10/95.

[27] van Leeuwen H. The determination of the pressure–viscosity coefficient of a lubricant through an accurate film thickness formula and accurate film thickness measurements. Proc Inst Mech Eng, Part J. 2009 12;223(8):1143–1163.

[28] Hamrock BJ, Schmid SR, Jacobson BO. Fundamentals of Fluid Film Lubrication. 2nd ed. Faulkner LL, editor. New York: Marcel Dekker, Inc.; 2004.

[29] Lugt PM, Morales-Espejel GE. A Review of Elasto-Hydrodynamic Lubrication Theory. Tribology Transactions. 2011;54(3):470–496. Available from: https://doi.org/10.1080/10402004.2010.551804.

[30] Dowson D, Higginson GR. Elastohydrodynamic lubrication, the fundamentals of roller and gear lubrication. Oxford: Pergamon Press; 1966.

[31] Johnson KL. Regimes of Elastohydrodynamic Lubrication. Journal of Mechanical Engineering Science. 1970;12(1):9–16. Available from: https://doi.org/10.1243/JMES_JOUR_1970_012_004_02.

[32] Hamrock BJ, Dowson D. Elastohydrodynamic lubrication of elliptical contacts for materials of low elastic modulus I—fully flooded conjunction. J of Lubrication Tech. 1978 Apr;100(2):236–245. Available from: https://doi.org/10.1115/1.3453152.

[33] Crook AW. The lubrication of rollers II. Film thickness with relation to viscosity and speed. Philosophical Transactions of the Royal Society of London Series A, Mathematical and Physical Sciences. 1961;254(1040):223–236.

[34] Grubin A. Fundamentals of the hydrodynamic theory of lubrication of heavily loaded cylindrical surfaces. Investigation of the Contact

Machine Componets. 1949;2.

[35] Wheeler JD, Fillot N, Vergne P, Philippon D, Morales-Espejel GE. On the crucial role of ellipticity on elastohydrodynamic film thickness and friction. Proc Inst Mech Eng, Part J. 2016 Mar;230(12):1503–1515. Available from: https://doi.org/10.1177/1350650116637583.